Cousins M. M., Briggs J., Whitwell T. (2017), Beach *Vitex* (*Vitex rotundifolia*): Medicinal properties, biology, invasive characteristics and management options. *Journal of Environmental Horticulture*, 35(4), 128-137. **16.** Yang X. Y., Gao P. Y., Chen X. X., Wang L. X., Jiang T., Wu T., Chen Y. Y., Yue C. Y., Wu H. W., Tang L. Y., Wang Z. J. (2023), Comparison of HPLC fingerprints and determination of main components of *Viticis* fructus from different species. *Zhongguo Zhong Yao Za Zhi*, 48(9), 2471-2479. **17.** Sun Y. Q., Zhao L. Y., Zhu B., Jia M., Zhang Q. Y., Qin L. P. (2021), Genetic diversity and genetic structures of original plants of *Viticis* fructus*: an SSR markers-based analysis. Zhongguo Zhong Yao Za Zhi*, 46(15), 3824-3831. **18.** Bramley G. L. C., Forest F., R. P. J. (2009), Troublesome tropical mints: Re-examining generic limits of *Vitex* and relations (Lamiaceae) in south east asia. *Taxon*, 58(2), 500-510. **19.** Do T. D. (2014), *Phương pháp xác định độc tính của thuốc*.NXB Y học. Hà Nội. **20.** Do T. D. (1997), Đánh giá mô hình gây phù thực nghiệm bằng cao lanh và carrageenan để nghiên cứu tác dụng chống viêm của thuốc. *Tạp chí Dược học*, 12, 18-20. **21.** Vogel H. G. (2002), Drug Discovery and Evaluation: Pharmacological Assays. *Springer Science & Business Media.* **22.** Vogel H. G. (2008), Drug Discovery and Evaluation: Pharmacological Assays. *Springer Science & Business Media.* (ed). **23.** Jain N. K., Patil C. S., Singh A., Kulkarni S. K. (2001), A simple technique to evaluate inflammatory pain along with anti-inflammatory studies in carrageenan-induced paw edema. *Indian Journal of Pharmacology*, 33(2), 114-115. **24.** Sugishita E., Amagaya S., Ogihara Y. (1981), Anti-inflammatory testing methods: comparative evaluation of mice and rats. *Journal of Pharmacobio-dynamics*, 4(8), 565-575. **25.** Annamalai P., Thangam E. B. (2022), *Vitex trifolia* L. modulates inflammatory mediators via down-regulation of the NF-κB signaling pathway in carrageenan-induced acute inflammation in experimental rats. *Journal of Ethnopharmacology*, 298, 115583. **26.** Wee H. N., Neo S. Y., Singh D., Yew H. C., Qiu Z. Y., Tsai X. R. C., How S. Y., Yip K. Y. C., Tan C. H., Koh H. L. (2020), Effects of *Vitex trifolia* L. leaf extracts and phytoconstituents on cytokine production in human U937 macrophages. *BMC Complementary Medicine and Therapies*, 20, 1-15. **27.** Matsui M., Adib-Conquy M., Coste A., Kumar-Roiné S., Pipy B., Laurent D., Pauillac S. (2012), Aqueous extract of *Vitex trifolia* L.(Labiatae) inhibits LPS-dependent regulation of inflammatory mediators in RAW 264.7 macrophages through inhibition of nuclear factor kappa B translocation and expression. *Journal of Ethnopharmacology*, 143(1), 24-32. **28.** Zheng C. J., Li H. Q., Ren S. C., Xu C. L., Rahman K., Qin L. P., Sun Y. H. (2015), Phytochemical and pharmacological profile of *Vitex negundo. Phytotherapy Research*, 29(5), 633-47. **29.** Yao J. L., Fang S. M., Liu R., Oppong M. B., Liu E. W., Fan G. W., Zhang H. (2016), A review on the terpenes from genus *Vitex. Molecules*, 21(9). **30.** Chan E. W. C., Wong S. K., Chan H. T. (2018), Casticin from *Vitex* species: A short review on its anticancer and anti-inflammatory properties. *Journal of Integrative Medicine*, 16(3), 147-152. **31.** Le D. D., Han S., Yu J., Ahn J., Kim C. K., Lee M. (2023), Iridoid derivatives from *Vitex rotundifolia* L. f. with their anti-inflammatory activity. *Phytochemistry*, 210, 113649. **32.** Ramakrishna R., Bhateria M., Singh R., Puttrevu S.K., Bhatta R. S. (2016), Plasma pharmacokinetics, bioavailability and tissue distribution of agnuside following peroral and intravenous administration in mice using liquid chromatography tandem mass spectrometry. *Journal of Pharmaceutical and Biomedical Analysis*, 125, 154-64. **33.** Kim J., Seo Y. H., Kim J., Goo N., Jeong Y., Bae H. J., Jung S. Y., Lee J., Ryu J. H. (2020), Casticin ameliorates scopolamine-induced cognitive dysfunction in mice. *Journal of Ethnopharmacology*, 259, 112843. **34.** Nerattini M., Jett S., Andy C., Carlton C., Zarate C., Boneu C., Battista M., Pahlajani S., Loeb-Zeitlin S., Havryulik Y., Williams S., Christos P., Fink M., Brinton R. D., Mosconi L. (2023), Systematic review and meta-analysis of the effects of menopause hormone therapy on risk of Alzheimer's disease and dementia. *Frontiers in Aging Neuroscience*, 15, 1260427.

Journal of Medicinal Materials, 2024, Vol. 29, No. 6 (pp. 377 - 384)

BINARY ETHOSOMES FOR ENHANCING SKIN DELIVERY OF RUTIN BY SOLVENT INJECTION

Nguyen Hong Van[1,*], Phan Huu Phuoc[1], Nguyen Xuan Tung[2]

[1]Life Sciences Department, University of Science and Technology of Hanoi, Hanoi, Vietnam

[2]VNU University of Medicine and Pharmacy, Vietnam National University, Hanoi, Vietnam

*Corresponding author: chodomthanyeu@gmail.com

(Received November 05th, 2024)

Summary

Binary Ethosomes for Enhancing Skin Delivery of Rutin by Solvent Injection

Rutin, a natural extract from buckwheat, tea, and apple, has powerful pharmacological properties, especially antioxidant effects. However, the bioactivity of rutin is limited since it has low solubility and poor permeability. Nanovesicles, especially ethosomes, have been a non-invasive drug carrier for skin delivery with high entrapment efficiency and stability. In this research, the simple solvent injection was used to fabricate classical ethosomes, and binary ethosomes. Various polyols, like propylene glycol, isopropyl alcohol, and glycerol at different ratios were investigated in rutin binary ethosome preparation. Then, rutin ethosomes were characterized by physical properties, loading efficiency, drug release, and short-term stability. The optimum binary ethosomes were made from the mixture of ethanol and glycerol at the ratio of 3:7. Rutin binary ethosomes had a lower size than classical ethosomes and better stability during 30 days. Rutin ethosomes posed sustained release through dialysis membrane and mouse skin and significantly improved the drug release in the Franz cell model. Therefore, binary ethosomes could be considered as potential nanovesicles to deliver rutin via the skin route.

Keywords: *Ethosomes, Classical ethosomes, Binary ethosomes, Skin delivery, Rutin.*

1. Introduction

Herbal medicines have been used to treat various diseases for thousands of years in history. In modern pharmaceutics, bioactive compounds and their derivatives, extracted from natural sources, have been recognized as new alternative drugs and supplements, to improve human health, cure, and prevent pathologies [1]. Rutin is a significantly familiar Vietnamese herbal compound, from *Sophora japonica L.*, and is traditionally used in daily life in the form of tea, food, and even as an active pharmaceutical ingredient in marketed drugs [2]. In terms of chemistry, rutin is a flavonol glycoside between quercetin and disaccharide rutinose. Rutin has activities of kidney protection, neuroprotection, hepatitis protection, inflammation, antidiabetic, anticancer, reducing blood pressure, etc. The bioactivity of rutin refers to its capabilities of regulating and signaling pathways involving gene expression, oxidative stress, apoptosis...[3],[4],[5]. In dermatology, bioactivities such as antioxidant, free-radical scavenging, oxidative-stress prevention, and collagen synthesis modulators enable rutin usage for skin anti-aging, and skin protection [6]. Moreover, rutin is antibacterial [7], wound-healing [8], skin-whitening [9], and UV protectant, and strengthens the UV-blocking ability of sun protection factor (SPF) agents [10], which has been widely applied in skin products. However, rutin and almost all bioactive natural substances have a high molecular weight, poor solubility, and low penetrability, which limit the permeation into skin layers.

Therefore, nanotechnology has been used in pharmaceutical preparations to make a number of botanical bioactive substances more bioavailable, target bioactive sites, and control drug release rate [1]. Several pharmaceutical ingredients from natural bioactive compounds, with applied nanotechnology, were approved by US-FDA and EMA [11]. For skin delivery, ethosomes have been considered as one of the most outstanding nanocarriers [12]. The combination of bilayer nanostructure, composed of phospholipid and ethanol, enables facile penetration of ethosomes into the skin layer, as well as improves the stability and deformity compared to liposomes (Fig. 1.) [13]. Ethanol in ethosomal structure causes two effects to enhance the penetration through the skin layer of active pharmaceutical ingredients (API) [14]. In the former effect, ethanol interacts with the hydrophobic head in the stratum corneum, which softens and loosens the stratum corneum layer. Consequently, APIs penetrate through the skin efficiently. In the latter effect, ethanol in vesicle structure improves the ability to fuse membranes, facilitating the process of API permeation into dermal and hypodermal cells. Ethosomes, with the involvement of other polyols, such as PG [12],[15], IPA [16], and glycerol [17], are called binary ethosome. Binary ethosomes have greater stability and drug permeability than classical ethosomes [15],[18]. Specifically, binary ethosomes increased 7 folds in permeability *ex-vivo*, and 1.5 fold in *in vivo* anti-inflammatory [15]. Additionally, blending propylene glycol in phloretin binary ethosomes raised the precutaneous permeability 1.06 folds more than classical ethosomes, and 2.4 folds than PG solution [19]. The major methods for ethosome preparation are thin film hydration [18] and solvent - injection [12]. Solvent - injection is a more advantageous method for ethosome fabrication due to the simple process and scale - up [20].

However, there have been a few studies on dermal nanovehicles loading rutin, including the ethosomal system. Candido and his colleagues [21] prepared a rutin ethosome with a size of 369 nm and a zeta potential (ZP) of -19.6 mV. In another study, the optimized rutin ethosome has a size of 112 nm and an entrapment efficiency (EE) of 67.5% [22]. Although previous studies suggested rutin ethosome had a better antioxidant than free rutin, the enhancement of rutin penetrability by ethosome still did not clarify. Moreover, the articles only presented the classical ethosome, while the latter ethosome generation may express more potential effectiveness. Therefore, research about rutin ethosomes should be carried out to improve the therapeutic treatment of this Vietnamese bioactive agent, specifically for skin delivery. Hence, this study aims to fabricate the more modern type of ethosome - binary ethosome by facile solvent injection method for improvement of the therapeutic effectiveness of rutin for dermal treatment.

2. Materials and methods

2.1. Materials

Rutin was an active pharmaceutical ingredient

(CAS 153-18-4). Ethanol was from Xilong Scientific Co., Ltd (China). Lecithin (>90% Phosphatidylcholine) was from Yuanye Biology, Shanghai (China). Propylene glycol (PG), isopropyl alcohol (IPA), and glycerol were from Xilong Scientific Co. Ltd (China).

2.2. Methods

2.2.1. Ethosome preparation:

Rutin ethosome samples were prepared following the solvent injection method with mild modifications [23],[24]. Firstly, rutin was dissolved in ethanol/polyols using a magnetic stirrer (IKA C-MAG HS 4). At 30ºC, lecithin was added and dissolved completely to form a homogeneous organic phase. Distilled water (aqueous phase) was added to the organic phase by a syringe pump (Perfusor Compact) at a constant rate of 300 µL/min. Then, the ethosomes were sonicated by a probe sonicator (Q-Sonica) at 50W, 45/15 seconds for pulse on/ pulse off time, in 5 minutes to obtain uniform ethosomes. Finally, the products were stored in closed glass vials for further studies (Fig. 1). Rutin was fixed at 2.5 mg/mL, various lecithin ratios of 3%, 1.5%, 0.5% (w/v), ethanol concentrations at 20%, 35%, 50% (v/v), and different polyols, including PG/IPA/Glycerol, were investigated to prepare ethosomes.

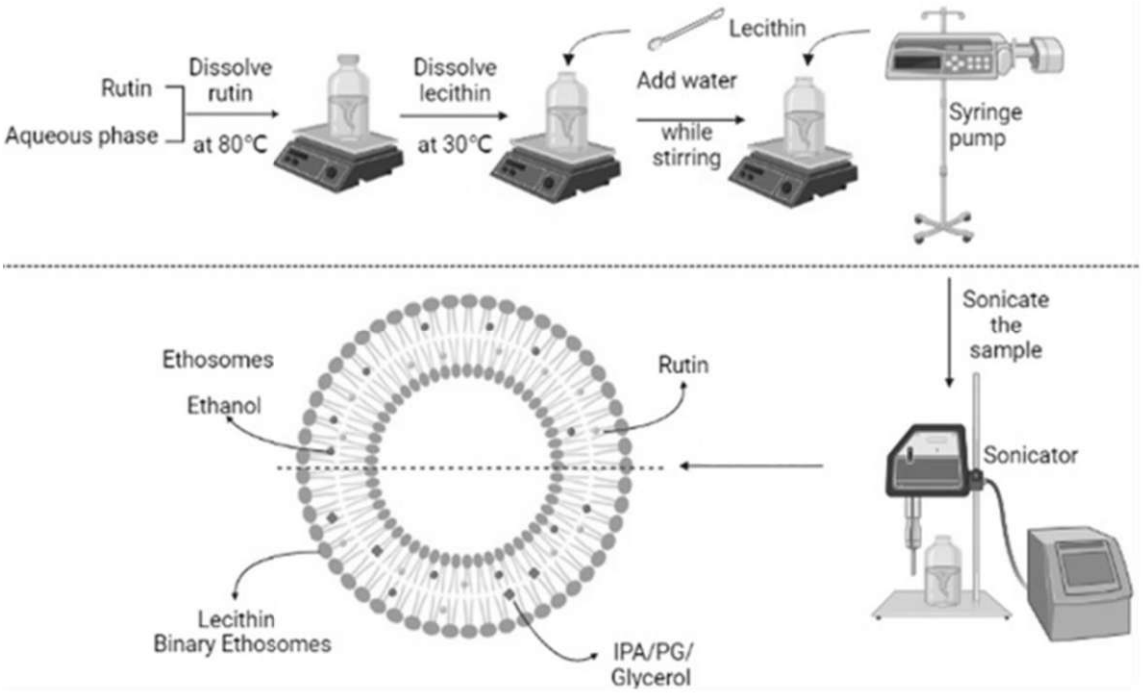

Fig. 1. Rutin ethosome fabrication

2.2.2. Size, polydispersity index, and zeta potential:

Size, polydispersity index (PDI), and zeta potential (ZP) of ethosome vesicles were measured by a nanoparticle analyzer (HORIBA nanoPartica SZ-100). Vesicle size was calculated based on the Stock - Einstein equation. ZP was calculated according to laser doppler electrophoresis (HORIBA Scientific 2023). Method setting included water as a medium, 4 opening cuvettes for size measurement, and carbon electrode zeta cuvettes for ZP measurement. Ethosome samples were diluted with water to ensure precise measurement when measuring size, PDI, and ZP.

2.2.3. Morphology:

The visualization of ethosome samples was investigated by transmission electron microscopy (TEM) (JEOL Inc, Jem - 1400).

2.2.4. Rutin quantification:

The quantification rutin was evaluated by an HPLC method [21]. The stationary phase was a C18 reversed-phase column (150 x 4.6 mm, 5 µm), while the mobile phase was mixed from acetic acid 1% and acetonitrile (80:20) with the flow rate of 1 mL/min, 355 nm (Thermo Scientific™, UltiMate™ 3000 Standard (SD) HPLC Systems).

2.2.5. Drug entrapment efficiency (EE):

EE was a value showing the content of rutin which was encapsulated in ethosomal vesicle according to the equation below:

$$EE = \frac{R_e}{R_t}.100\% = \frac{R_t - R_f}{R_t}.100\%$$

Where Re is encapsulated rutin, R_f is free rutin, R_t is the total content of rutin.

To determine free rutin content, the ultrafiltration method was applied with a 10000 Da cutoff at the speed of 10.000 rpm in 15 min. The rutin in the filtrate was quantified by HPLC.

2.2.6. Stability test:

Rutin ethosomes were stored in various conditions: at 4°C, at 25°C at a relative humidity of 60%, for 30 days to check the change in physical properties, like size, PDI, ZP, and EE.

2.2.7. Drug release study:

The penetration ability of rutin ethosome formulations was investigated by an experiment using Franz vertical diffusion cells. A dialysis membrane/or mouse skin was placed in the joint to separate the donor and receptor chambers. A volume of samples containing 5 mg rutin was added into a donor compartment. In the receptor compartment, a phosphate buffer pH 6.8 was filled to mark and stirred at a fixed rate. The temperature of the receptor compartments was kept at 37°±0.5°C during the experiments. At time interval points, a fixed volume of medium was collected to determine rutin concentration by the HPLC method.

2.2.8. Data analysis:

T-test and one-way ANOVA test to evaluate statistical significance (setting at $p < 0.05$) were performed with Microsoft Excel. Data was reported as average ± standard deviation (SD). A value of $p < 0.05$ was considered statistically significant (*). Each experiment was carried out in triplicate.

3. Results and discussion

3.1. Effect of different concentrations of lecithin on rutin ethosome properties

The ratios of phospholipid bases strongly affected the size and PDI of ethosomes (Fig. 2A). At 3% (w/v) of lecithin, the size is 201.45 ± 0.15 nm, larger than that of 1.5%, 190.32 ± 3.56 nm, and 0.5%, 161.07 ± 0.89 nm. Conversely, the ethosome homogeneity at 0.5% lecithin was marginally better than that of 1.5% and 3% concentrations, as the PDI was 0.13 and around 0.25, respectively. The ZP is used to quantify the charge of the vesicles, of which the parameter reflects the stability of the formulation. The lower the lecithin ratios, the higher the absolute value of ethosome ZP [25]. At 3%, 1.5%, and 0.5% of the lecithin concentration, the charges were -13.76 ± 0.32, -20.09 ± 0.45, and -24.13 ± 1.21, respectively. The absolute value of ZP in the range of 20-30 mV could be considered acceptable for supporting the stability of these nanovesicles. Based on the physical properties, 0.5% of lecithin (w/v) was chosen for further experiments.

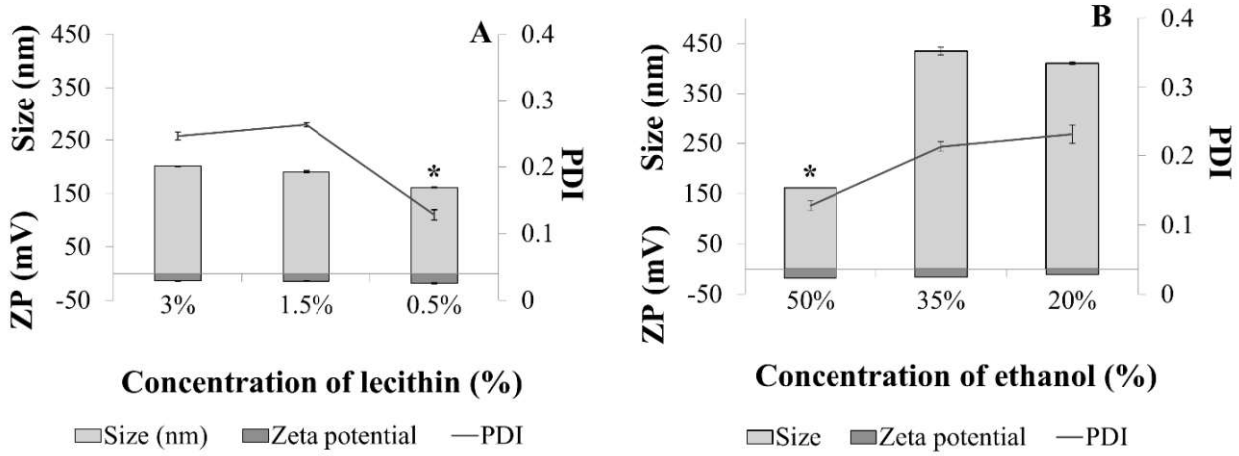

Fig. 2. Rutin ethosome physical properties at different lecithin ratios (w/v) and ethanol concentrations (v/v), 2A. Lecithin ratios, 2B. Ethanol ratios

3.2. Effect of different concentrations of ethanol on rutin ethosome properties

Formulations of ethosomes were evaluated with the different ratios of ethanol: 50%, 35%, and 20% (v/v) (Fig. 2B). With 20% ethanol, the nanoparticle size was 410.57 ± 5.08 nm, significantly larger than that of 50% ethanol, 161.0 ± 0.89 nm. The ethanol concentrations affected ethosome size, as the higher the ethanol concentration, the lower the ethosomal size [25]. At higher concentrations of ethanol (55% and 60%), the ethosomal vesicles disappeared, confirmed by the abnormal size value (under 20nm) and higher PDI (above 0.4), agreed with previous studies [13]. Hence, the 50% ethanol (v/v) was chosen for the rutin ethosome. When compared to pure rutin (about 21.23 µm), and other rutin ethosomes by the same method, the resulting ethosomes in this study had a smaller size. In other research, the size of the ethosomal nanoparticle was 634.9nm (without sonication) [26], and rutin-loaded ethosomes, prepared by the thin-film hydration method, had the size of 247 ± 7 nm or 369.5 ± 4.2 nm [27].

3.3. Effect of other polyols in binary ethosomes

Different types of polyols were used to prepare rutin binary ethosomes with various blended ratios of ethanol: polyols at 3:7, 5:5, and 7:3 (Fig. 3) Other polyols could be considered as permeability enhancers and stabilizers [25].

3.3.1. Effect of propylene glycol in binary ethosomes:

The higher the PG ratios in rutin binary ethosomes, the smaller the size, in agreement with the previous study [25]. At ratios 7:3, 5:5, and 3:7 ratio of ethanol to propylene glycol, rutin ethosomal size reduced from above 350 nm to around 140 nm. In another study, optimum nicotine ethosomes containing ethanol: PG at the ratio of 5:5 were productive transdermal delivery systems [12]. In the case of PG, all rutin binary ethosomes had the PDI in the preferable range (PDI < 0.3). The binary ethosomes with PG exhibited ZP value in the acceptable range to prevent agglomeration. In addition, increasing PG quantities decreased the ethosomal ZP from -20.5 ± 0.47 mV to -23.8 ± 0.70 mV. Hence, ethanol: PG at the ratio of 7:3 had the smallest size, 137.7 ± 0.40 nm, and the best homogeneity.

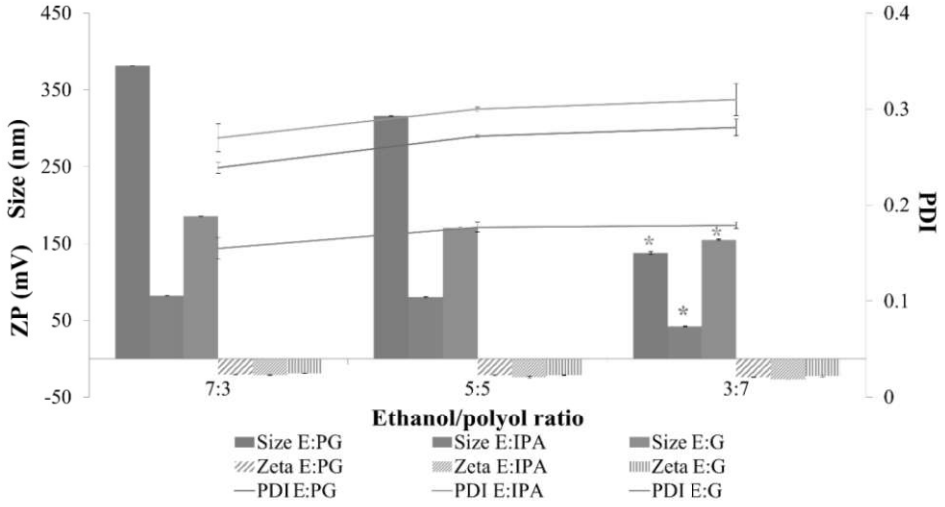

Fig. 3. Binary ethosomes at different ethanol/polyol ratios
E: ethanol, PG: propylene glycol, IPA: isopropanol alcohol, G: glycerol

3.3.2. Effect of isopropyl alcohol in binary ethosomes:

The second polyol investigated in rutin binary ethosomes formulation was isopropyl alcohol (Fig. 3.). With mixtures of ethanol and IPA, at any ratios, the size of the ethosome significantly reduced, compared to solely ethanol. Noticeably, at the blend ratio of 7:3 of ethanol: IPA, the nanovesicle size dropped from above 160 nm to only 42.31 ± 0.85 nm. Conversely, the PDI increased considerably in the presence of IPA in ethosomes, from below 0.2 in classical ethosomes, up to around 0.3. Moreover, the presence of IPA increased the negative charge in the ZP of ethosomes.

3.3.3. Effect of glycerol in binary ethosomes:

The third polyol studied for rutin binary ethosomes was glycerol (Fig. 3.). The presence of glycerol in the binary ethosomes caused a slight decrease in nanovesicular size from 185.58 ± 0.55 nm (ethanol: glycerol = 7:3) to 155.09 ± 1.76 nm (ethanol: glycerol = 3:7), which demonstrated the effect of glycerol on particle size reduction. Furthermore, the PDI of all three formulations revealed a uniform size, with a PDI of less than 0.2. The increase in ZP with glycerol strengthened the stability of the rutin binary ethosome.

Among the three investigated polyols, IPA induced the greatest reduction in the size of binary ethosomes, as the size went down 4 folds related to classical ethosomes. However, in consideration of uniformity, the involvement of glycerol resulted in better PDI, below 0.2. Almost all rutin ethosomes had a high EE, more than 90%. Therefore, the alcohols for rutin binary ethosomes should be the mixture of ethanol and glycerol at the ratio of 3:7, with a size of 155.16 ± 1.76, PDI of 0.18 ± 0.01, ZP of -22.61 ± 2.46 mV, and EE of 92.41 ± 0.08% with the spherical shape shown in TEM images (Fig. 4.). In comparison with meloxicam ethosomes, 169 nm, 0.2 PDI, and 83.1 EE%, rutin binary ethosome could be considered successfully prepared and had better physical properties and drug loading [15].

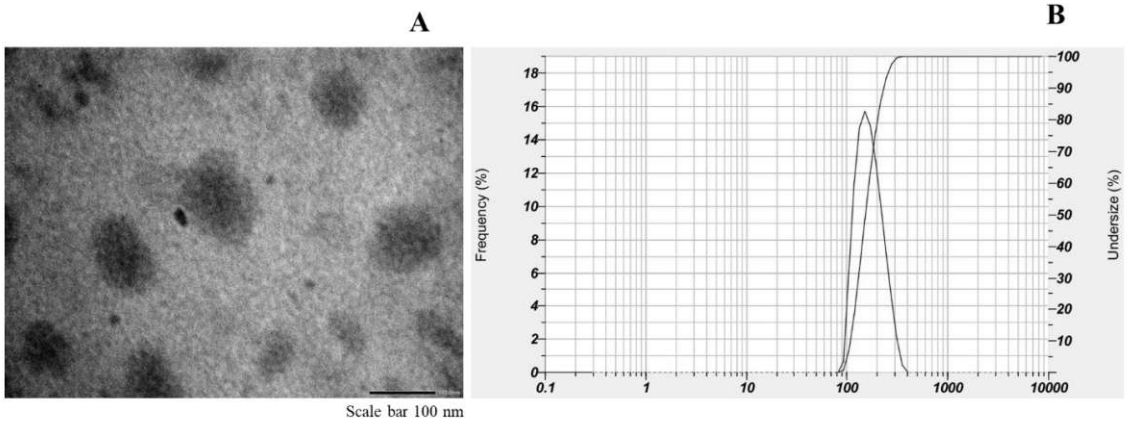

Fig. 4. TEM image and size distribution histogram of rutin binary ethosomes with glycerol
A. TEM image, B. size distribution histogram

3.4. Stability test

Initial investigation on the stability of rutin ethosomes was carried out in 30 days at 4°C and 25°C. The changes in size, PDI, ZP, and EE of classical ethosomes and binary ethosomes were presented in Table 1. There were significant increases in the size and PDI of all ethosomes in both tested temperatures. The size of the glycerol binary ethosomes rose from above 150 nm to approximately 200 nm after 30 days. Additionally, the PDI gained from 0.18 ± 0.01 to 0.23 ± 0.01 after 30 days at 25°C. Also, the absolute value of ZP slightly decreased from nearly 23 mV to about 20 mV after 30 days. In particular, the changes in physical characteristics and EE of various types of ethosomes at 4°C were slower than at 25°C. For example, after 30 days, the size of classical ethosomes at 4°C was considerably smaller than that at 25°C, 221.03 ± 0.08 nm, and 320.04 ± 1.87 nm, respectively. Moreover, the EE of binary ethosomes with glycerol slightly fell from 92.41± 0.08 to 89.17 ± 0.15 after 30 days at 4°C. These observations suggested that storage in a colder environment provides better stabilization for rutin ethosomes.

The stability of rutin ethosomes could be improved by using combinations of ethanol and PG, IPA, and glycerol. In particular, after 30 days at 25°C, the size of classical ethosomes increased 2 folds from 161.02 ± 0.89 nm to 320.04 ± 1.87, while for binary ethosomes with glycerol, the size only gained 1.2 times, from 155.09 ± 1.76 nm to 202.82 ± 1.27 nm. These results suggested the combination of polyols stabilized the ethosome structures more than using solely ethanol.

Table 1. Size, PDI, ZP, and EE of binary ethosomes after 15 days and 30 days

Freshly preparation	**Size (nm)**	**PDI**	**ZP (mV)**	**EE (%)**
Classical ethosomes	**161.02 ± 0.89**	**0.13 ± 0.02**	**-24.16 ± 1.21**	**90.89 ± 0.05**
Binary ethosomes with glycerol	**155.09 ± 1.76**	**0.18 ± 0.01**	**22.61 ± 2.46**	**92.41± 0.08**
4ºC -15 days				
Classical ethosomes	201.02 ± 0.08	0.22 ± 0.03	-16.58 ± 2.96	**87.91 ± 0.10**
Binary ethosomes with glycerol	*190.82 ± 1.91*	*0.21 ± 0.01*	*-20.86 ± 1.96*	**90.40 ± 0.10**
4ºC -30 days				
Classical ethosomes	221.03 ± 0.08	0.33 ± 0.06	-13.72 ± 1.98	**79.96 ± 0.02**
Binary ethosomes with glycerol	*200.35 ± 1.26*	*0.22 ± 0.01*	*-20.64 ± 0.01*	**89.17 ± 0.15**
25ºC -15 days				
Classical ethosomes	290.05 ± 0.08	0.29 ± 0.04	-15.51 ± 1.91	**85.56 ± 0.02**
Binary ethosomes with glycerol	*200.92 ± 0.81*	*0.22 ± 0.36*	*-20.13 ± 0.64*	**89.96 ± 0.05**
25ºC -30 days				
Classical ethosomes	320.04 ± 1.87	0.376 ± 0.08	-12.63 ± 1.48	**79.06 ± 0.01**
Binary ethosomes with glycerol	*202.82 ± 1.27*	*0.23 ± 0.01*	*-19.21 ± 0.07*	**86.93 ± 0.03**

3.5. In-vitro rutin release

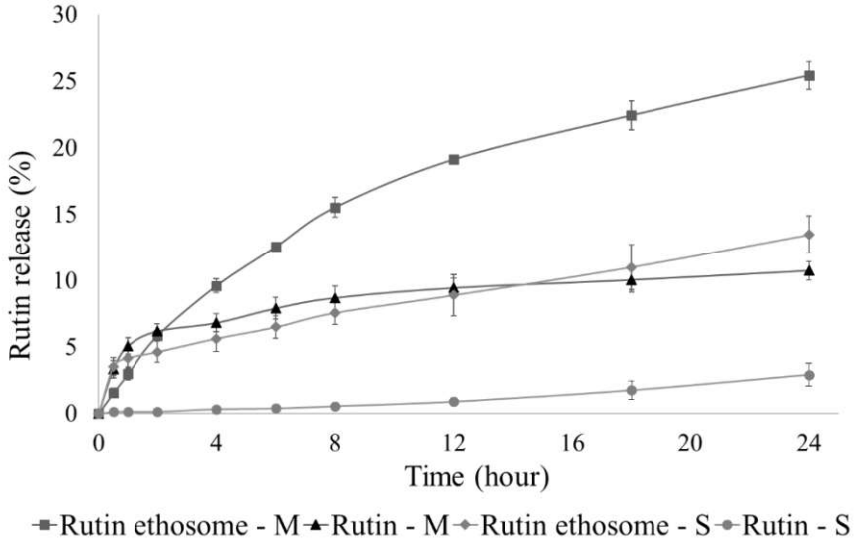

Fig. 5. Rutin release profile from binary ethosomes with glycerol
S- mouse skin, M- dialysis membrane

The rutin release was evaluated through the Franz-cell model, through mouse skin and dialysis membrane, from binary ethosomes with glycerol (Fig. 5.). Generally, in both mouse skin and dialysis membrane, ethosomes also expressed sustained releases. Additionally, ethosomes improved the permeability of rutin not only through the dialysis membrane but also through mouse skin. Specifically, after 24 hours, rutin released more than 2.5 folds through mouse skin and nearly four folds through the dialysis membrane than rutin itself. Therefore, binary ethosomes were effective nanocarriers to enhance drug delivery through the skin, as confirmed by a previous study [28].

4. Conclusion

Rutin ethosomes and binary ethosomes were successfully fabricated. The optimum formulation was the mixture of ethanol and glycerol at the ratio of 3:7, the total volume of polyols at 50% (v/v), lecithin at 0.5% (w/v) and rutin at a final concentration of 2.5 mg/mL. These binary ethosomes had a size above 150 nm and were homogenous (PDI<0.2). Besides, the ZP absolute value was greater than 30 mV and the EE was at around 92%. Additionally, the physical properties and drug loading hardly changed during 30 days at 4ºC. Moreover, these rutin binary ethosomes exhibited sustained release and improved the

permeability of the drug through the dialysis membrane as well as mouse skin during 24 hours. Hence, rutin binary ethosomes may be considered as potential drug delivery systems for skin anti-aging, skin healing, and furthermore.

Declaration of Competing Interest: *The authors report no conflicts of interest.*

Acknowledgment: *This research received funding from University of Science and Technology of Ha Noi (USTH) under Grant Agreement No [USTH.LS.01/24].*

References

1. Watkins R., Wu L., Zhang C., Davis R. M., Xu B., (2015), Natural product-based nanomedicine: recent advances and issues, *International Journal of Nanomedicine*, 10, 6055-74. **2.** Habtemariam S., Varghese G. K., (2015), Extractability of rutin in herbal tea preparations of *Moringa stenopetala* leaves, *Beverages*, 1(3), 169-182. **3.** Enogieru A. B., Haylett W., Hiss D. C., Bardien S., Ekpo O. E., (2018), Rutin as a potent antioxidant: implications for neurodegenerative disorders, *Oxidative Medicine and Cellular Longevity*, 2018(1), 6241017. **4.** Negahdari R., Bohlouli S., Sharifi S., Dizaj S. M., Saadat Y. R., Khezri K., Jafari S., Ahmadian E., Jahandizi N. G., Raeesi S., (2020), Therapeutic benefits of rutin and its nanoformulations, *Phytotherapy Research*, 35(4), 1719-1738. **5.** Satari A., Ghasemi S., Habtemariam S., Asgharian S., Lorigooini Z., (2021), Rutin: a flavonoid as an effective sensitizer for anticancer therapy; insights into multifaceted mechanisms and applicability for combination therapy, *Evidence-Based Complementary and Alternative Medicine*, 2021(1), 9913179. **6.** Choi S. J., Lee S. N., Kim K., Joo D. H., Shin S., Lee J., Lee H. K., Kim J., Kwon S. B., Kim M. J., Ahn K. J., An I. S., An S., Cha H. J., (2016), Biological effects of rutin on skin aging, *International Journal of Molecular Medicine*, 357-363. **7.** Ivanov M., Novović K., Malešević M., Dinić M., Stojković D., Jovčić B., Soković M., (2022), Polyphenols as inhibitors of antibiotic resistant bacteria—mechanisms underlying rutin interference with bacterial virulence, *Pharmaceuticals*, 15(3), 385. **8.** Chen L. Y., Huang C. N., Liao C. K., Chang H. M., Kuan Y. H., Tseng T. J., Yen K. J., Yang K. L., Lin H. C., (2020), Effects of rutin on wound healing in hyperglycemic rats, *Antioxidants*, 9(11), 1122. **9.** Jo Y. J., Yoo D. H., Lee I. C., Lee J., Jeong H. S., (2022), Antioxidant and skin whitening activities of sub-and super-critical water treated rutin, *Molecules*, 27(17), 5441. **10.** Tomazelli L. C., de Assis Ramos M. M., Sauce R., Cândido T. M., Sarruf F. D., de Oliveira Pinto C. A. S., de Oliveira C. A., Rosado C., Velasco M. V. R., Baby A. R., (2018), SPF enhancement provided by rutin in a multifunctional sunscreen, *International Journal of Pharmaceutics*, 552(1-2), 401-406. **11.** Rahman H., Othman H., Hammadi N., Amin K., Samad A. N., Alitheen N., (2020), Novel drug delivery systems for loading of natural plant extracts and their biomedical applications, *International Journal of Nanomedicine*, 15, 2439-2483. **12.** Wang H., Shao Q., Zhang Y., Ding J., Yang M., Yang L., Wang W., Cui P., Dai Z., Ma L., (2024), Preparation and evaluation of liposomes containing ethanol and propylene glycol as carriers for nicotine, *Current Drug Delivery*, 21(2), 249-260. **13.** Abdulbaqi I. M., Darwis Y., Khan N. A. K., Abou Assi R., Khan A. A., (2016), Ethosomal nanocarriers: the impact of constituents and formulation techniques on ethosomal properties, *in vivo* studies, and clinical trials, *International Journal of Nanomedicine*, 11, 2279. **14.** Sherin F., Saju F., Jagadeesh A., Syamasree S., Paul N., Venugopal A., (2019), Ethosome: A novel approach to enhance drug permeation, *International Journal of Pharmaceutical Sciences Review and Research*, 55(1), 18-22. **15.** Al-Ameri A. A. F., Al-Gawhari F. J., (2024), Formulation development of meloxicam binary ethosomal hydrogel for topical delivery: *in vitro* and *in vivo* assessment, *Pharmaceutics*, 16(7), 898. **16.** Sayed O. M., Abo El-Ela F. I., Kharshoum R. M., Salem H. F., (2020), Treatment of basal cell carcinoma via binary ethosomes of vismodegib: *in vitro* and *in vivo* studies, *Aaps Pharmscitech*, 21, 1-11. **17.** Sharma D., Rani A., Singh V. D., Shah P., Sharma S., Kumar S., (2023), Glycerosomes: novel nano-vesicles for efficient delivery of therapeutics, *Recent Advances in Drug Delivery and Formulation*, 17(3), 173-182. **18.** Hamzah M. L., Kassab H. J., (2024), Formulation and characterization of intranasal drug delivery of frovatriptan-loaded binary ethosomes gel for brain targeting, *Nanotechnology, Science and Applications*, 1-19. **19.** Zhang M., Zhuang X., Li S., Wang Y., Zhang X., Li J., Wu D., (2023), Designed fabrication of phloretin-loaded propylene glycol binary ethosomes: stability, skin permeability and antioxidant activity, *Molecules*, 29(1), 66. **20.** Wang J., He W., Cheng L., Zhang H., Wang Y., Liu C., Dong S., Zha W., Kong X., Yao C., (2022), A modified thin film method for large scale production of dimeric artesunate phospholipid liposomes and comparison with conventional approaches, *International Journal of Pharmaceutics*, 619, 121714. **21.** Cândido T. M., Camila A. D. O., Maíra B. A., Maria V. R. V., Catarina R., André R. B., (2018), safety and antioxidant efficacy profiles of rutin-loaded ethosomes for topical application, *American Association of Pharmaceutical Scientists*, 19, 1773-80. **22.** Cristiano M. C., Barone A., Mancuso A., Torella D., Paolino D., (2021), Rutin-loaded nanovesicles for improved stability and enhanced topical efficacy of natural compound, *Journal of Functional Biomaterials*, 12(4), 74. **23.** Somwanshi S. B., (2019), Development and evaluation of novel ethosomal vesicular drug delivery system of *Sesamum indicum* L. seed extract, *Asian Journal of Pharmaceutics*, 12(4), 1290. **24.** Andleeb M., Shoaib Khan H.M., Daniyal M., (2021), Development, characterization and stability evaluation of topical gel loaded with ethosomes containing *Achillea millefolium* L. extract, *Frontiers in Pharmacology*, 12, 336. **25.** Aljohani A. A., Alanazi M. A., Munahhi L. A., Hamroon J. D., Mortagi Y., Qushawy M., Soliman G. M., (2023), Binary ethosomes for the enhanced topical delivery and antifungal efficacy of ketoconazole, *OpenNano*, 11, 100145. **26.** Dhiman A., Singh D., Fatima K., Zia G., (2019), Development of rutin ethosomes for enhanced skin permeation, *International Journal of Traditional Medicine and Applications*, 1, 4-10. **27.** Cândido T. M., De Oliveira C. A., Ariede M. B., Velasco M. V. R., Rosado C., Baby A. R., (2018), Safety and antioxidant efficacy profiles of rutin-loaded ethosomes for topical application, *Aaps Pharmscitech*, 19(4), 1773-1780. **28.** Jiang D., Jiang Y., Wang K., Wang Z., Pei Y., Wu J., He C., Mo X., Wang H., (2022), Binary ethosomes-based transdermal patches assisted by metal microneedles significantly improve the bioavailability of carvedilol, *Journal of Drug Delivery Science and Technology*, 74, 103498.